Graphical Abstract

New Facilities for the Production of 1 mm gap Resistive Plate Chambers for the Upgrade of the ATLAS Muon Spectrometer

F. Fallavollita, O. Kortner, H. Kroha, P. Maly, G. Proto, D. Soyk, E. Voevodina, J. Zimmermann, on behalf of the ATLAS Collaboration

Highlights

New Facilities for the Production of 1 mm gap Resistive Plate Chambers for the Upgrade of the ATLAS Muon Spectrometer

F. Fallavollita, O. Kortner, H. Kroha, P. Maly, G. Proto, D. Soyk, E. Voevodina, J. Zimmermann, on behalf of the ATLAS Collaboration

- Strategic Industrial Collaborations to Enhance RPC Production for ATLAS Muon Spectrometer Upgrade

- Innovative and Scalable Manufacturing Techniques for High-Rate Resistive Plate Chambers

- Comprehensive Certification Process Validates Readiness for High-Luminosity LHC Deployment

New Facilities for the Production of 1 mm gap Resistive Plate Chambers for the Upgrade of the ATLAS Muon Spectrometer

F. Fallavollita[a,*], O. Kortner[a], H. Kroha[a], P. Maly[a], G. Proto[a], D. Soyk[a], E. Voevodina[a], J. Zimmermann[a], on behalf of the ATLAS Collaboration

[a]*Max Planck Institut für Physik , Boltzmannstr. 8, Garching, 85748 , Bavaria, Germany*

Abstract

The ATLAS Muon Spectrometer is set for a significant upgrade as part of the High-Luminosity LHC (HL- LHC) program, which includes the installation of three additional full coverage layers of new generation thin-gap Resistive Plate Chambers (RPCs) in the inner barrel region. These RPCs feature a reduced gas gap thickness of 1 mm between high-pressure phenolic laminate (HPL) electrodes, enhancing their background rate capability and longevity. This upgrade aims to maximize the muon trigger acceptance and efficiency. To achieve this, nearly 1000 RPC gas gaps need to be produced. To mitigate reliance on a single supplier and expedite production, the ATLAS muon community has partnered with two new companies in Germany and the Max Planck Institute for Physics in Munich. The gas gap assembly procedure was adapted to the infrastructure and tools available at the industrial manufacturers, facilitating the transfer of technology to industry after the prototyping phase. The certification of the manufacturers was achieved by constructing several small- and full-size RPC gas gap prototypes at each facility. The prototypes underwent rigorous testing at CERN's Gamma Irradiation Facility (GIF++), where their efficiency and time resolution were measured under different gamma background levels. The performance of these prototypes met the requirements for ATLAS at the HL-LHC. Additionally, the prototypes successfully passed an accelerated aging test at the GIF++, where they were exposed to the maximum photon dose expected during HL-LHC operations. This contribution will present the gas gap manufacturing proce-

---

*Corresponding Author: fallavol@mpp.mpg.de

dures, the results of the certification tests, and the comparative analysis of the production methods investigated to ensure the reliability and efficiency of RPC production at external companies. The outcomes demonstrate that the new facilities are capable of producing high-quality RPCs according to the industrial standards.

1. New facilities for scalable production of RPC detectors

In response to the growing demand for high-rate Resistive Plate Chambers (RPCs) in high-energy physics experiments, new large-scale production facilities and methods have been developed. These advanced RPCs feature a 1 mm gas volume with high-pressure phenolic laminate (HPL) electrodes, providing enhanced background rate capability and longevity, essential for experiments like those at the High-Luminosity LHC (HL-LHC) and beyond [1]. To ensure high-quality, efficient production, a dedicated assembly and certification facility has been established at the Max Planck Institute for Physics in Munich, supported by strategic collaborations with two German industrial manufacturers, PTS® and MIRION® companies. This partnership enabled the seamless transfer of advanced assembly techniques from research to industry, incorporating innovations such as automated precision assembly lines and rigorous quality control protocols embedded within the production workflow to ensure both scalability and compliance with stringent ATLAS performance standards. The prototyping and certification process followed a structured, phased approach to systematically prepare for large-scale production of the gas volumes, ensuring compliance with stringent industrial standards [2]. In the initial phase, the developments have been based on the production procedures initially employed by the ATLAS and CMS experiments for their RPC detector technology. These procedures have been subsequently refined to facilitate production at an industrial scale. The optimized procedure has been implemented on $40 \times 50 \, cm^2$ small-scale RPC detector prototypes, demonstrating its scalability and applicability to full-scale RPCs with final dimensions of $1.0 \times 2.0 \, m^2$. These small-scale detector prototypes played a crucial role in assessing both performance and manufac-

turing quality, offering valuable insights into the production and certification process. The collaboration is now advancing toward the final certification phase, which encompasses comprehensive testing of both small- and large-scale RPC detector prototypes, with a strong focus on longevity studies, including a year-long irradiation test at CERN's Gamma Irradiation Facility (GIF++). This phase is pivotal in confirming that the selected manufacturers meet the stringent qualifications essential for large-scale production. This article will detail the novel assembly methods, the successful technology transfer to industrial partners, and the capacity of the new facilities to deliver high-quality RPCs on an industrial scale, ensuring readiness for high-energy physics applications beyond the HL-LHC upgrade.

2. Test-beam studies of the small-scale RPC detector prototypes

As part of the qualification process for large-scale production of RPC gas volumes for the ATLAS Muon Spectrometer upgrade, small-scale 1 mm gap RPC detector prototypes ($40 \times 50 \, cm^2$) have been successfully manufactured by the PTS® and MIRION® companies. In dedicated test-beam campaigns at CERN GIF++ facility, these prototypes have been subjected to comprehensive performance evaluations under conditions simulating the operational environment, with exposure to a $\sim$11 TBq ^{137}Cs source, emitting 662 keV gamma rays, in combination with a 100 GeV muon beam from the secondary SPS beam line H4 [3]. In the following, the main RPC detector prototype performances is reported in terms of muon detection efficiency, time resolution and absorbed current. For the standard ATLAS-RPC gas mixture (94.7% $C_2H_2F_4$: 5% $i - C_4H_{10}$: 0.3% SF_6), the results are compared at different levels of irradiation, expressed by means of the gamma cluster rate as measured at the detector working point of 5.8 kV. The dependencies of relevant variables are presented as functions of the effective high voltage, V_{eff}, which is defined by the expression:

$$V_{eff} = V_{app} \times \frac{P_0}{P} \times \frac{T}{T_0} \tag{1}$$

where V_{app} is the applied high voltage, P represents the atmospheric pressure, and T the temperature at the time of data-taking. The constants P_0 = 990 mbar and T_0 = 293 K correspond to the average pressure and temperature conditions observed at the GIF++ facility. Further details and technical aspects regarding the experimental setup and analysis of test beam

data obtained with small-scale RPC detector prototypes, produced by German manufacturers, are provided in [4]. The following results validate the high manufacturing standards achieved by the German PTS® and MIRION® companies, underscoring their technical readiness to advance to large-scale production that fulfills the stringent performance and reliability requirements of the ATLAS Muon Spectrometer upgrade.

2.1. Muon Detection Efficiency

The muon detection efficiency is evaluated as the number of events where at least one cluster has been detected inside the muon window divided by the total number of triggers. The efficiency as a function of V_{eff} is shown in Figure 1b for the standard ATLAS-RPC gas mixtures at different gamma cluster rates evaluated at the detector working point. The efficiency dependency on V_{eff} has been interpolated by means of the sigmoid functions:

$$\epsilon = \frac{\epsilon_{max}}{1 + e^{-\lambda(V_{eff} - V_{50\%})}} \qquad (2)$$

where the parameter ϵ_{max} represents the maximum plateau efficiency, $V_{50\%}$ is the V_{eff} at 50% of the maximum efficiency and λ is proportional to the slope of the efficiency curve at $V_{50\%}$. The gap RPC detector prototypes, operated with the standard gas mixture at the working point, demonstrated an average muon detection efficiency of approximately 97% under source-off conditions. When exposed to medium particle rates, reaching up to $\sim 1.5\,kHz/cm^2$, this efficiency showed a slight reduction of about 3%. At higher rates, up to $\sim 3.0\,kHz/cm^2$, a more pronounced degradation was observed, with efficiency decreasing by around 8% and accompanied by a progressive shift in the working point toward higher values. Despite the rate-dependent effects observed, the RPC detector prototypes demonstrated considerable resilience, achieving a muon detection efficiency greater than 96.5% at the nominal operating voltage under HL-LHC -like background conditions (~ 200–$300\,Hz/cm^2$).

2.2. Time Resolution

The absolute time resolution of the RPC detector prototypes has been evaluated using the Time-of-Flight (TOF) method by measuring the difference in signal arrival times between pairs of detectors selected from a set of three. All possible detector combinations have been analyzed, consistently yielding comparable results, thereby validating the reliability and

4

reproducibility of the measurements. The absolute time resolution has been determined by dividing the estimated time difference resolution by $\sqrt{2}$, under the assumption that both the detectors and electronic components of both detectors are identical and their contributions are uncorrelated. The width of time difference distributions $\langle \sigma_{\Delta t} \rangle$ is extracted using a Gaussian function and the absolute time resolution $\langle \sigma_t \rangle$ is given by:

$$\langle \sigma_t \rangle = \frac{\langle \sigma_{\Delta t} \rangle}{\sqrt{2}} \tag{3}$$

A preliminary result for the time difference distribution between signals generated by the same muons in two strips in two parallel gap RPC detector prototypes in coincidence is shown in Figure 1c. The standard deviation of the signal time difference distribution has been measured to be 573 ± 13 ps, corresponding to an absolute time resolution of 405 ± 9 ps for 100 GeV muon beam, well within the ATLAS requirement of 1 ns, demonstrating excellent timing performance of the prototypes.

2.3. Gas Gap Current

A critical operational limitation of RPC detectors under irradiation is managing the current flowing through the gas volume. Excessive current could lead to potential damage, emphasizing the need for close monitoring to ensure the long-term reliability and safety of RPC detectors in high-radiation environments. To address this, current flow within the gas volume has been systematically monitored during both in-spill and out-of-spill data acquisition phases. Out-of-spill data has been specifically utilized to assess the average current, allowing for an evaluation of its mean value and associated statistical uncertainty. The current has been determined by measuring the voltage drop across a 100 kΩ resistor connecting one of the two HPL plates to ground. The absorbed currents as a function of the effective high voltage applied across the gas volume for standard ATLAS-RPC gas mixtures under different irradiation conditions are presented in Figure 1d. The findings indicate an overall increase in the average current, correlated with both higher effective voltage levels and increased irradiation rates.

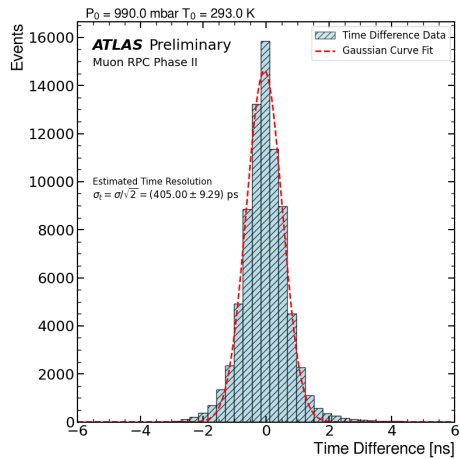## 3. Assembly methodology for a full-scale RPC gas volume

In this section, the production process for full-scale 1 mm gap RPCs are detailed, with particular emphasis on modifications implemented to streamline and enhance manufacturability in an industrial environment.
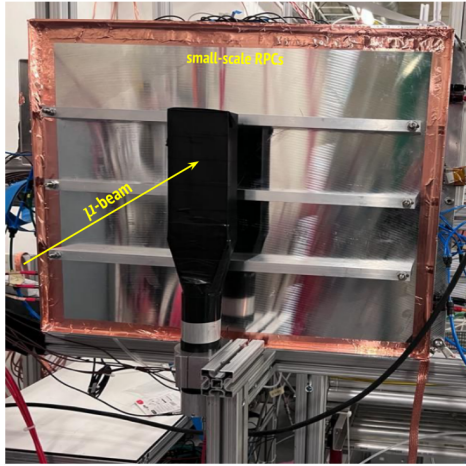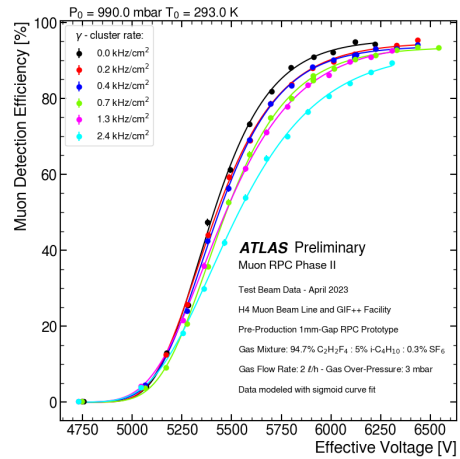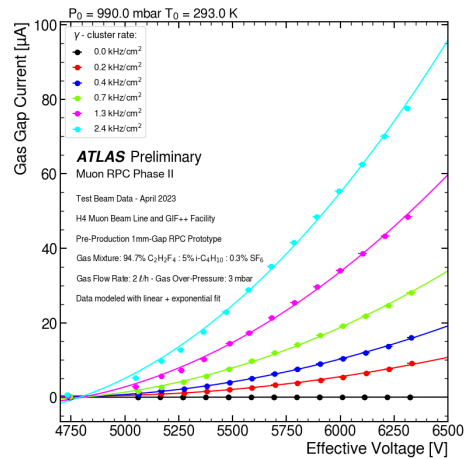
Figure 1: (a) Photograph of the experimental setup installed at the CERN GIF++ facility. (b) Muon detection efficiency as a function of effective high voltage for the standard gas mixture. The efficiency data points are interpolated by a sigmoid function. (c) Time difference distribution and time resolution results of the beam test. The blue line shows the distribution of the time difference and the red line is obtained from the gaussian fitting. (d) Current as a function of the effective high voltage. Results are shown at different gamma cluster rates evaluated at the detector working point.

3.1. Manufacturing Process of High-Pressure Laminate Electrodes

The RPC gas volume comprises two High Pressure Laminate (HPL) plates, each manufactured from multiple layers of kraft paper impregnated with phenolic resin. These plates are sourced from the Italian manufacturer Teknemica® with strict quality specifications: the nominal thickness is specified as 1.40 mm, with a tolerance of +0.10 mm and -0.07 mm, while the tolerance on linear dimensions is ±0.5 mm. Additionally, to maintain uniformity and structural stability, the difference between the two diagonals is required to be less than 1 mm. The HPL plates feature a bulk resistivity range of $1.5 \times 10^{10} \, \Omega \, cm$ to $6 \times 10^{10} \, \Omega \, cm$, measured at $20°C$ and 50% relative humidity, providing the necessary electrical characteristics for efficient detector operation and performance [1], [5]. A precise graphite coating is applied to the external surfaces of the HPL plates to ensure consistent high-voltage distribution across the electrodes. This graphite layer, critical for the detector performance [1], [5], has strict quality specifications: its surface resistivity is required to be 320 $k\Omega/\square$, with a tolerance of ±30%, to maintain reliable operation under high-voltage conditions. The application of this graphite varnish is achieved through a silk-screen printing process manufactured by the German company Siebdruck Esslinger®, which has proven to be the most reliable method for meeting the specified surface resistivity across all electrodes. A copper contact strip is attached to the graphite-coated surface of the HPL electrodes with conductive silver adhesive to ensure optimal electrical connectivity. For effective electrical insulation in the HPL electrodes, a polyethylene terephthalate (PET) foil is laminated onto the graphite-coated surfaces of the electrodes. This insulation step involves bonding a 190 μm thick PET foil, coated with 80 μm thick low-melt ethylene vinyl acetate (EVA), to each electrode using a laminating pressing machine set to $105°C$ with lamination speed of $\sim 3 \, m/min$. Figure 2a and 2b show the laminating press machine and the HPL electrode upon the completion of the lamination process, respectively.

3.2. Manufacturing Process of Gas Volume

The two HPL electrodes are separated by mechanically precise polycarbonate spacers, ensuring an accurately defined gas volume width. The mechanical precision required for the spacer thickness, with a tolerance of ±15 μm, is achieved through injection molding. To prevent gas volume variations exceeding 15 μm, which could result from non-uniform glue thickness
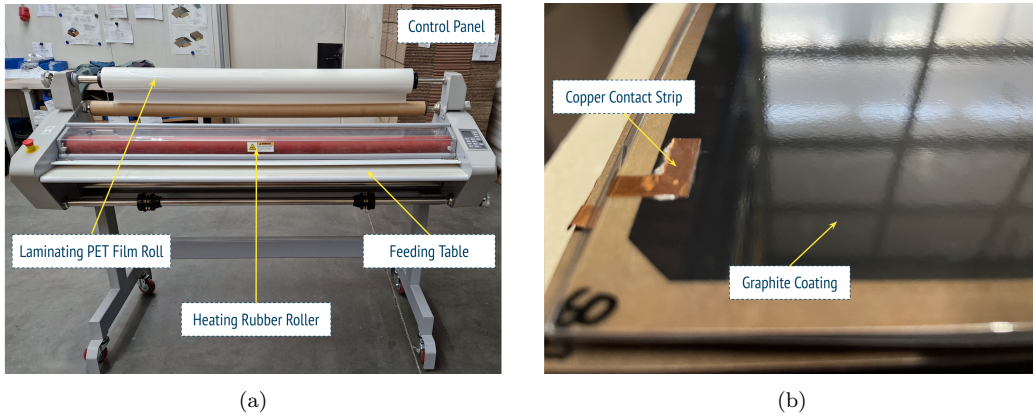
Figure 2: (a) Lamination press machine for the application of PET foil to graphite-coated HPL electrodes for electrical insulation. (b) HPL electrode following the completion of the PET lamination process.

securing the spacers onto the HPL plates, and to ensure a consistently defined glue layer, a cross-shaped dimple was introduced into the spacer design, as shown in Figure 3a. Additionally, gas tightness is maintained by a poly-carbonate lateral profile bonded along the perimeter, which also interfaces with the gas distribution system. The assembly of the gas volume demands precise timing, particularly when applying epoxy glue to bond poly-carbonate spacers and lateral profiles to the resistive electrodes. Given the limited working time of approximately 50 minutes, this phase introduces additional complexity, requiring careful coordination to achieve accurate alignment and secure bonding within the time constraints. To decouple the precise positioning of spacers, approximately 400 components per full-size gas volume, from the gluing process, a dedicated template has been developed, as shown in Figure 3b This template comprises a Teflon plate with meticulously arranged slots and grooves, designed to accommodate both the spacers and lateral profiles. The Teflon plate is mounted on an aluminum frame equipped with a vacuum-based suction system, ensuring the secure placement of spacers and profiles during glue application and subsequent electrode alignment and positioning. Teflon has been chosen as the template material due to its non-stick properties, which prevent adhesive adherence and facilitate easy removal after assembly.

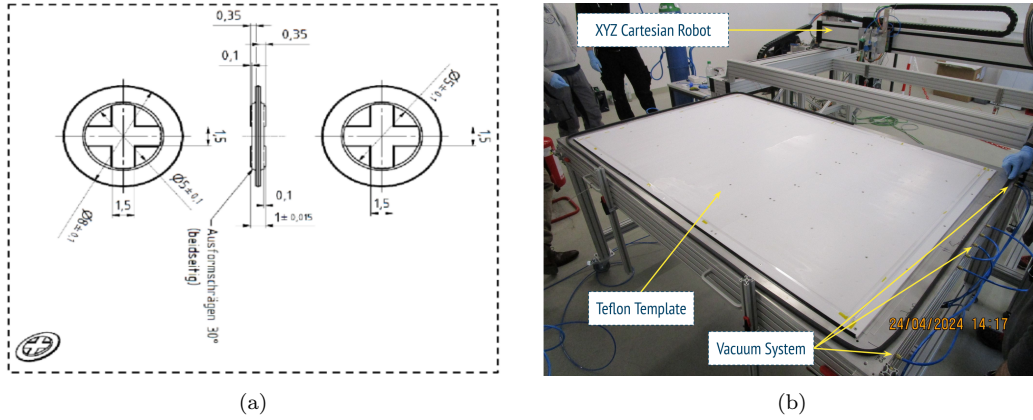<div style="text-align:center">(a)   (b)</div>

Figure 3: (a) Technical drawing of the polycarbonate spacer, featuring stringent mechanical tolerances on thickness to ensure precise fitting. The crosswise dimple design establishes a controlled and reproducible adhesive gap, facilitating accurate and consistent assembly. (b) Teflon template used for precise positioning of poly-carbonate spacers and lateral profiles prior to gluing them onto the HPL resistive electrode.

3.2.1. Gluing of the electrodes onto the spacers and lateral profiles

Following the precise placement of spacers and lateral profiles on the Teflon template, an automated glue dispenser, integrated with an XYZ Cartesian positioning systems, applies epoxy glue with high accuracy. The glue dispensing parameters, including dispensing pressure and time, and needle size, have been optimized to ensure the precise delivery of approximately $5\,\mu l$ of glue for each spacer and to compensate for the increase in glue viscosity over time. This configuration ensures uniform and controlled glue distribution across all components, significantly improving assembly precision and structural integrity. Figures 4a and 4b show the freeze frames capturing the glue dispensing process during the assembly phase.

The first HPL electrode plate is aligned and positioned onto the polycarbonate spacers and lateral profiles, and the vacuum bagging system is employed to maintain consistent pressure across the assembly, as shown in Figure 5a and Figure 5b. This step is critical for achieving uniform adhesion during the curing phase of the epoxy glue. The vacuum bagging system operates at a vacuum level of approximately -200 mbar, corresponding to a force of $\sim$100 N applied on each spacer. The curing process for the epoxy glue is carried out over a period of approximately 14 hours at a controlled temperature of 20-25$°C$ to ensure optimal bonding and structural stability.
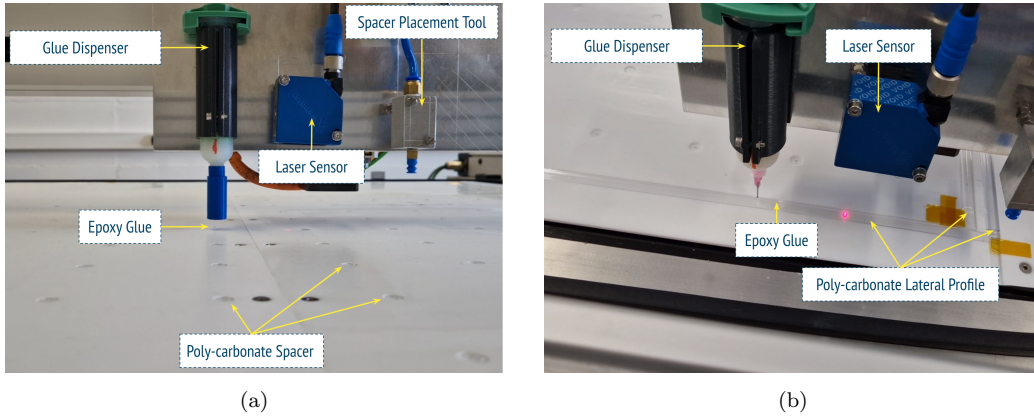
<div style="text-align:center">9</div>

Figure 4: (a) and (b) Freeze frames capturing the glue dispensing onto the spacers (left) and along the lateral profiles (right) of the gas volume.

After the overnight curing phase is complete, the vacuum is shut down, and the first electrode is removed from the vacuum bagging system. The Figure 5c shows the fully assembled first HPL electrode, with all poly-carbonate components, including the spacers and lateral profiles, firmly adhered to its surface.

The first HPL electrode plate, with the attached poly-carbonate spacers and lateral profiles, is carefully positioned on the assembly table and secured by a vacuum system. The epoxy glue is applied to the spacers and lateral profiles, following the same protocol as in the preliminary gluing phase, as shown in Figure 6a. Subsequently, the second HPL electrode plate is meticulously aligned and placed on top of the spacers and later profiles, as shown in Figure 6b. To ensure uniform pressure distribution, the assembly is compressed using a vacuum bagging system and maintained under pressure for a period of 14 hours, allowing sufficient time for the adhesive to fully cure and achieve optimal bonding strength, as shown in Figure 6c.

3.2.2. High-Voltage Cable and Gas Pipes Installation

Following the gluing of the gas volume, an 18 kV rated high-voltage cable is soldered to the copper contact strip, which has been previously affixed to the graphite-coated surface of the electrodes using a conductive silver adhesive, as shown in 7a. The gas pipes are connected to the gas volume through openings drilled into a lateral profile glued to the short side of the gas volume, as shown in Figure 7b. Each corner is equipped with a gas pipe,
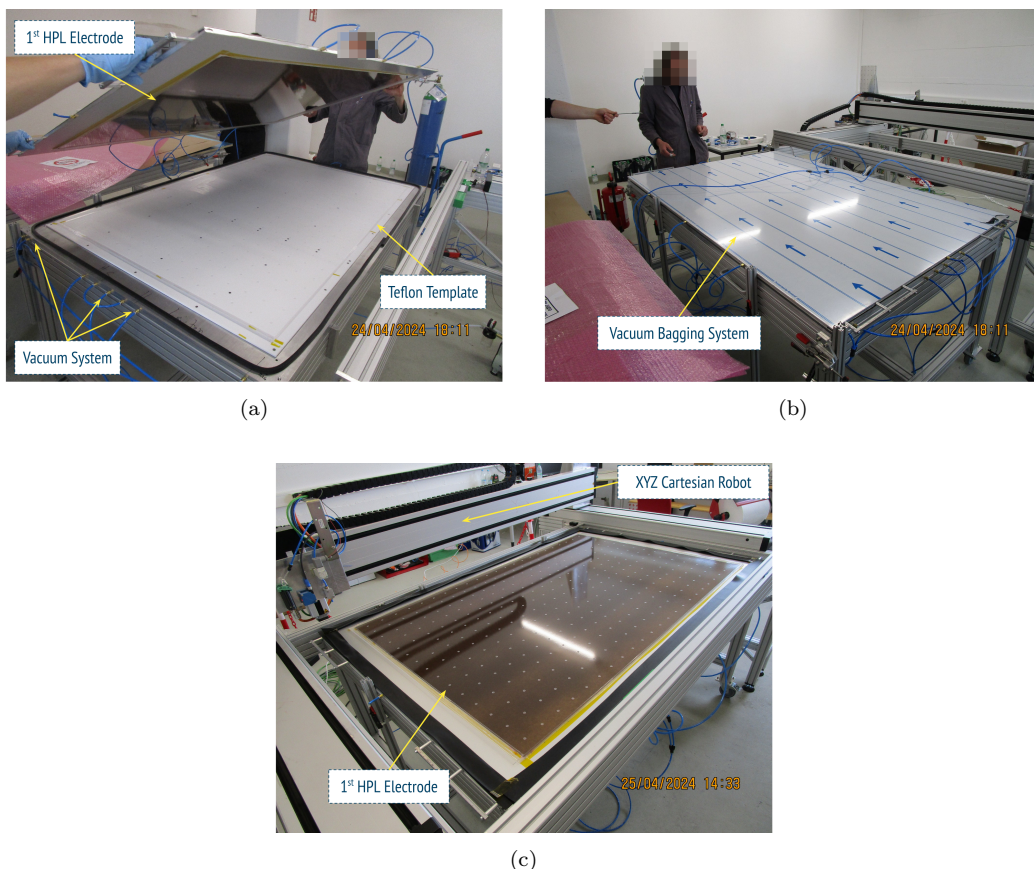
Figure 5: (a) Alignment and positioning of the first HPL electrode plate onto the poly-carbonate spacers and lateral profiles. (b) Vacuum bagging system employed to ensure consistent pressure across the entire assembly during the curing process. (c) Fully assembled HPL electrode with all poly-carbonate components firmly adhered to the surface.

and an internal distribution system has been designed to ensure uniform gas flow across the active volume of the detector.

3.2.3. Hot-Melt Glue Application and Spacer Indicator Installation

In the final construction process for the gas volume structure, the long sides are filled and sealed using EVA hot-melt glue applied with a gluing gun, as shown in Figure 8a. Teflon-coated aluminum bars are used during this step to ensure that the hot-melt glue does not increase the thickness of the gas volume along the edges, maintaining the integrity and uniformity of the gap size. The installation of spacer indicators on both surfaces of the RPC gas vol-
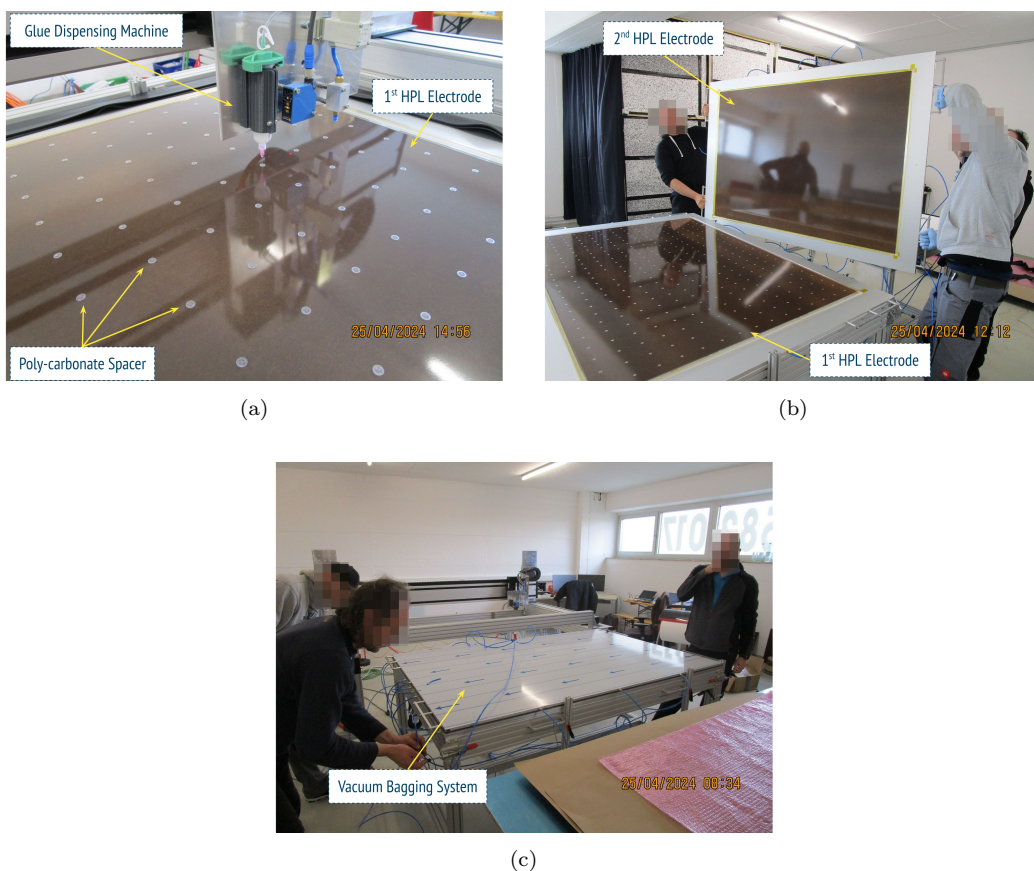
Figure 6: (a) Dispensing adhesive onto spacers and lateral profiles previously affixed to the HPL electrode. (b) Alignment and positioning of the second HPL electrode plate onto the poly-carbonate spacers and lateral profiles. (c) Vacuum bagging system employed to ensure consistent pressure across the entire assembly during the curing process.

ume is achieved by applying 0.10 mm-thick paper indicators, which provide supplementary reference points for accurately determining spacer positions, as shown in Figure 8b. The application process is fully automated, ensuring high throughput and precise positioning, which are crucial for maintaining stringent quality standards during the mass production of gas volume.

3.3. Linseed Oil Surface Treatment

The internal surfaces of HPL electrodes are treated with a thin layer of linseed oil, which significantly enhances the performance and reliability of the detectors. The oil treatment improves the electrode surface quality by
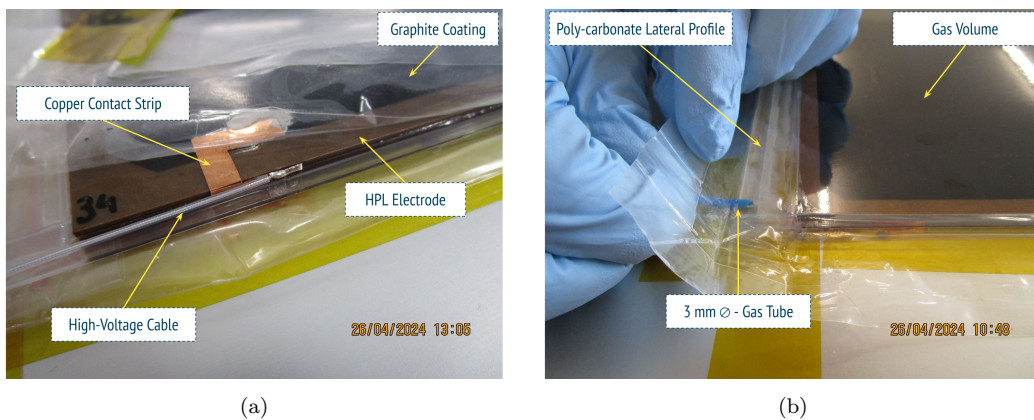
Figure 7: (a) Installation of the high-voltage cable soldered to the copper contact strip on the graphite-coated electrode. (b) Gas tube installation through openings in the lateral profile. Gas tubes are positioned at each corner for uniform gas distribution.
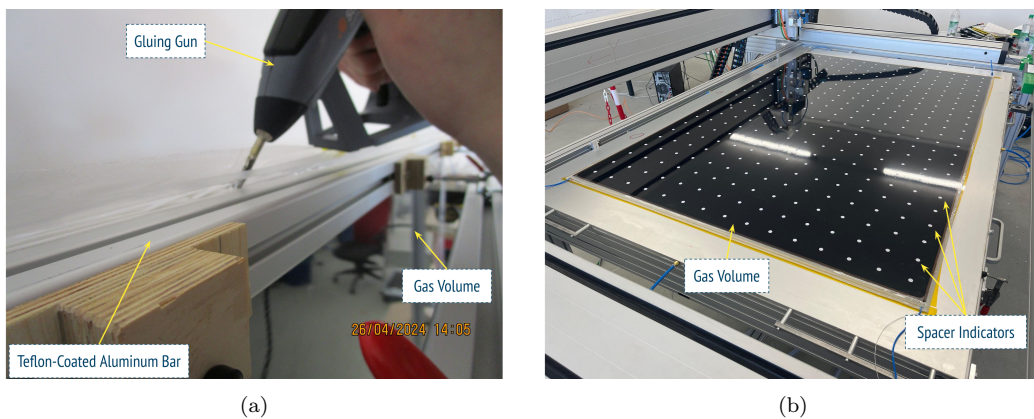

Figure 8: (a) Application of EVA hot-melt glue along the long sides of the gas volume structure. (b) Installation of 0.10 mm-thick paper indicators on gas volume surfaces to precisely determine spacer positions.

creating a smoother and more homogeneous layer, thereby reducing surface irregularities that could lead to localized high electric fields, increased intrinsic current, and elevated noise rates. Furthermore, linseed oil acts as an effective quencher for ultraviolet (UV) photons produced during gas ionization processes, thereby reducing secondary electron emissions and improving the overall stability of the detector. This combination of surface enhancement and photon quenching makes linseed oil treatment a critical step in the fabrication of RPC gas volumes, ensuring optimal detector performance and

13

extended operational lifespan. The standard procedure previously employed by the ATLAS and CMS Collaborations has been refined to achieve optimal results in the linseed oil treatment [1], [6]. The process starts by filling the gas volume with a carefully prepared mixture of 30% linseed oil and 70% heptane, which is introduced through the gas connections from a supply bottle. The heptane is used to reduce the viscosity of the oil, facilitating an even distribution. The operation is carried out in a temperature-controlled environment maintained at $30°C$ to ensure optimal conditions for the coating process. Additionally, in order to prevent blowouts under oil pressure, the gas volume is compressed between two rigid plates, with the entire assembly inclined at an angle of 30°, as shown in Figure 9. Following the filling process, the linseed oil is drained by progressively lowering the supply bottle at a controlled rate of approximately 1 m/h. This gradually draining process is imperative to prevent the formation of droplets and streaks, thereby preserving the uniformity of the linseed oil coating and ensuring the operational reliability of the gas volume. Finally, filtered air is circulated through the gas volume for a duration of two weeks to facilitate the complete polymerization of the linseed oil coating. During the initial 24 hours, the flow rate is controlled at 1 l/h to prevent any potential damage to the freshly applied linseed oil layer. Following this initial stabilization period, the flow rate is increased to 2 l/h, accelerating the polymerization process of the linseed oil varnish. This extended conditioning phase ensures thorough polymerization, resulting in a robust and uniform coating on the internal surfaces.
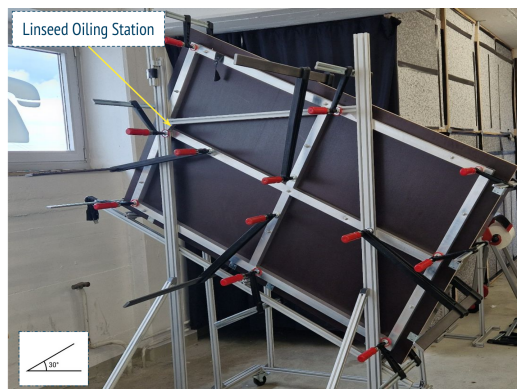

Figure 9: Oiling station for treating the internal surfaces of the gas volume with linseed oil.

4. Factory Acceptance Tests

To ensure the highest standards of quality and reliability in RPC gas volume production, a comprehensive Quality Assurance (QA) and Quality Control (QC) program has been established. This program encompasses a series of rigorous protocols and guidelines designed to rigorously monitor and verify every stage of the production process, from material selection and component assembly to final testing and certification.

4.1. Gas gap mechanical tests

The mechanical tests aim to verify the gas volume tightness and ensure the secure bonding of spacers between the HPL plates. While significant precautions are taken during fabrication, spacers could still detach due to inadequate glue bonding. Additionally, improper handling during assembly can further contribute to spacer detachment, emphasizing the importance of thorough testing to confirm structural integrity.

4.1.1. Spacer tensile strength measurement

The spacer tensile strength measurement is designed to assess the mechanical reliability of glued pillars on HPL plates, which are essential for ensuring the structural integrity of assembled gas volumes. To conduct this test, a $3 \times 3\,cm^2$ HPL-spacer-HPL sandwich sample is prepared from each gas volume at the end of each gluing phase. An initial traction force of 30 N is applied to each sample to verify the adhesion strength; if no detachment occurs, the force is then incrementally increased to determine the sample's breaking point. In standard tests, the breaking point is generally observed at traction forces exceeding 100 N, demonstrating a strong bond between the HPL plates and spacer pillars. This bond strength is critical for maintaining the integrity of the gas volume under operational conditions. Figure 10 illustrates the test stand employed to assess the tensile strength of spacer pillars, validating the mechanical integrity and robustness of adhesive joints on HPL plates.

4.1.2. Spacer height measurement

During the gas volume gluing process, maintaining precise spacer height is essential for achieving the required gas volume dimensions, which are critical for optimal detector performance. A quality control step was implemented to verify spacer height as an indirect measure of gas volume accuracy, thereby
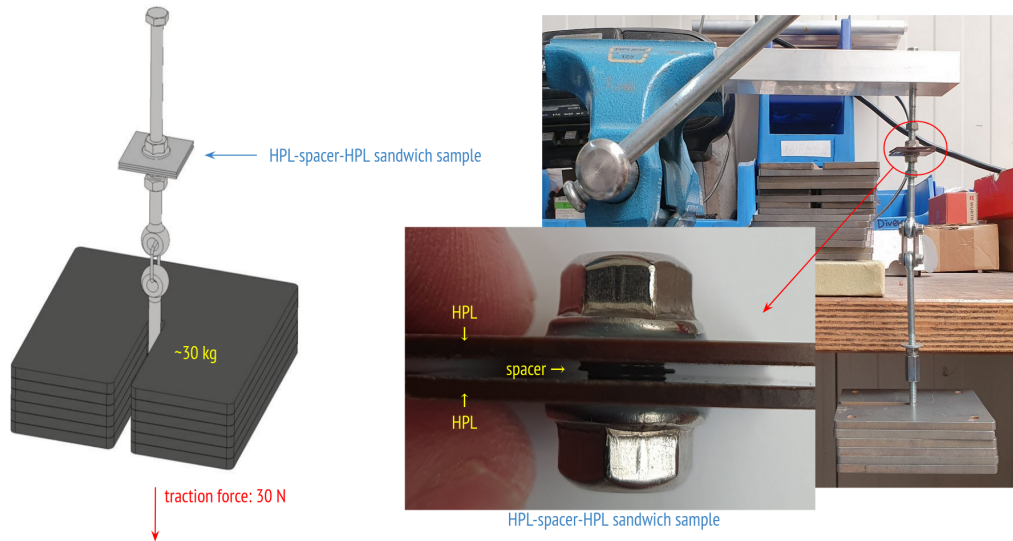
Figure 10: Schematic 3D model and photograph of the test stand for spacer tensile strength measurement on the $3 \times 3 \, cm^2$ HPL-spacer-HPL sandwich sample.

ensuring the required precision. After the initial adhesive application, the spacers remain accessible, enabling precise height measurements relative to the HPL plates. These measurements are conducted with a high-resolution digital drop indicator, which allows for an accurate assessment of compliance with the 1 mm gas volume specification. Analysis of the measured heights confirms that all spacers meet the gap specification, with deviations confined to a narrow range, remaining well within 20 μm. This minimal variation highlights the reliability of the gluing process, ensuring consistent gas volume dimensions throughout the assembly and contributing to the overall stability and reliability of the detector's performance. Representative test results from the spacer height measurement for a full-scale RPC gas volume prototype are presented in Figure 11.

4.1.3. Gas tightness measurement

The gas tightness test serves as the primary quality control step for newly assembled full-size Resistive Plate Chamber (RPC) gas volumes. This test detects potential leaks and quantifies the leak rate by monitoring the rate of internal over-pressure drop over time. Gas leaks are detrimental, as they waste gas and introduce external contaminants, humidity, and pollutants that can compromise detector performance by triggering reactions in the
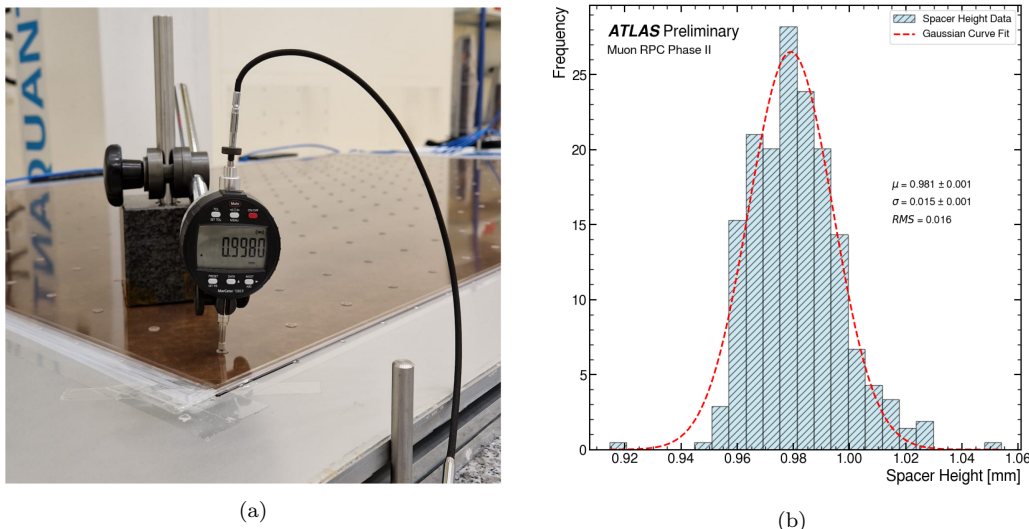
16

Figure 11: Spacer height measurement for a full-scale RPC gas volume prototype. (a) Photograph of the test stand for spacer height measurements. (b) One-dimensional histogram of spacer height measurements. The blue line shows the distribution of the spacer height measurements and the red line is obtained from the gaussian fitting.

active gas volume, leading to polymerization and, ultimately, performance degradation. A schematic of the gas system is shown in Figure 12. The setup connects the gas inlet to an argon (Ar) gas source with a pressure regulator. A one-way flow valve at the inlet controls the gas flow rate into the gas volume, while a differential manometer (RS PRO RS-8890) monitors inlet over-pressure. To prevent over-inflation, a safety bubbler vents gas flow at a set threshold (3.0–3.2 mbar above atmospheric pressure). Solenoid valves isolate the detector from the gas system during the measurement, and a high-precision pressure transducer (Baratron AA06A14TRB) records the internal over-pressure. This transducer is connected to a microprocessor-based unit (MKS Type 670B) for power, signal conditioning, and display. Ambient temperature and humidity sensors are positioned near the test stand to account for environmental factors.

The test procedure involves pressurizing the gas volume to approximately 3 mbar above atmospheric pressure with pure Ar gas. Pressure is recorded digitally to ensure precision, with QA/QC standards set by the ATLAS Muon Collaboration requiring a pressure loss not exceeding 0.1 mbar over a 3-minute period. After this phase, the gas leak rate is calculated to charac-
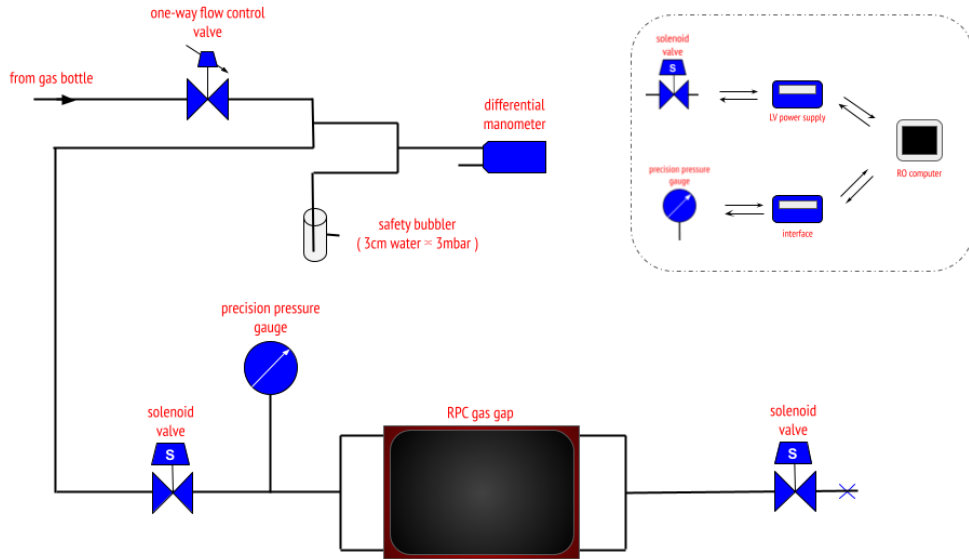
Figure 12: Diagram of the gas distribution system for leak tightness measurement.

terize the pressure decay rate. Once testing is complete, pressure is carefully released to ambient levels. For acceptance, the gas leak rate must be below $9.7 \times 10^{-4} \, mbar \times \ell/s$, corresponding to a 0.1 mbar pressure loss over 3 minutes for a gas volume of approximately 1.74 liters. This stringent criterion ensures long-term reliability and performance of each RPC gas volume in the ATLAS Muon Spectrometer upgrade. Representative test results from the gas tightness measurement are presented in Figure 13.

4.1.4. Mechanical rigidity measurement

Following successful gas leak testing, each full-size RPC gas volume undergoes a mechanical rigidity test to confirm structural integrity. This test verifies the robustness of adhesive bonds and handling quality achieved during fabrication, with a particular focus on detecting any detached spacers. The test utilizes a two-stage laser scanning method. First, a baseline planarity assessment is conducted at atmospheric pressure using a laser scanner, establishing an initial structural profile of the gas volume. Next, the gas volume is subjected to a slight overpressure of approximately 3 mbar, and a second laser scan is performed. This controlled increase in pressure highlights detachment issues that might not be visible at atmospheric pressure. The analysis process involves calculating the discrepancies between the laser
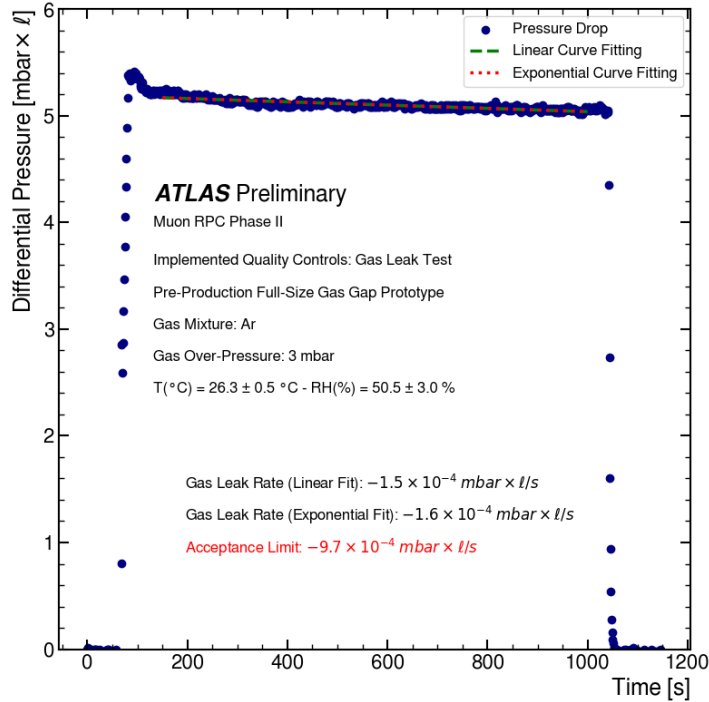
18

Figure 13: Results from the gas tightness measurement conducted on a full-size RPC gas volume. The experimental data have been analyzed using both linear and exponential regression models to accurately determine the gas leak rate.

scans taken at atmospheric and pressurized conditions. This comparative analysis is essential for identifying any significant changes or deviations that could indicate structural weaknesses. Through detailed examination of these discrepancies, areas of concern are precisely identified, allowing for corrective measures to reinforce the gas volume's integrity during the assembly procedure. This rigorous testing protocol is essential for maintaining the high standards necessary for the ATLAS Muon Spectrometer upgrade. Representative results from the mechanical rigidity measurement are presented in Figure 14.

4.2. Leakage current test

The leakage current test serves as a critical quality assurance step to verify the insulation integrity of the High Pressure Laminate (HPL) electrodes within each RPC gas volume. Ensuring proper insulation is essential to both
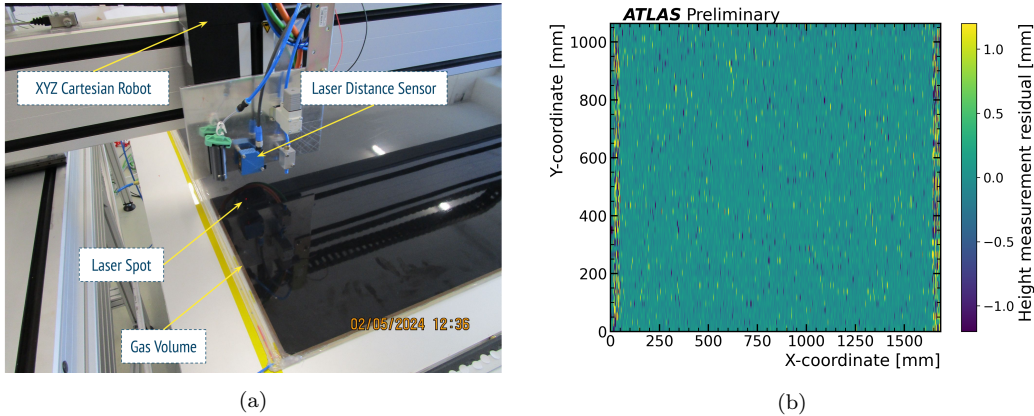
Figure 14: (a) Photograph of the test stand for the mechanical rigidity measurement of the gas volume. (b) Two-dimensional histogram of height measurement residuals for the mechanical rigidity assessment of a full-scale gas volume.

the safety and performance of the RPC detectors. During this test, a high voltage of up to 8 kV is applied to the HPL electrodes. A grounded, copper-coated aluminum bar is then placed in contact with the long side of the gas volume, connected through a 100 kΩ resistor to allow any leakage current to flow to ground. The leakage current is determined by measuring the voltage drop across the resistor with a digital multimeter, providing a sensitive indication of current leakage, as shown in Figure 15.

To comply with quality standards, the leakage current must remain below 200 nA at maximum applied voltage. This strict threshold ensures robust insulation quality of each gas volume, minimizing the risk of electrical failures that could compromise detector reliability and safety. Representative results from the leakage current test are presented in Figure 16.

4.3. Volt-Amperometric characteristic test

Each RPC gas volume is characterized by recording the Volt - Amperometric characteristic curve, which details the relationship between applied high voltage and the dark current (gap current). This test is conducted with the standard ATLAS-RPC gas mixture (94.7% $C_2H_2F_4$: 5% $i - C_4H_{10}$: 0.3% SF_6). The gap current comprises two main components: an ohmic current that flows through the Bakelite electrodes, spacers, and frame, and an avalanche-induced current generated within the gas. The voltage scan is conducted by gradually increasing the applied voltage in 200 V increments up
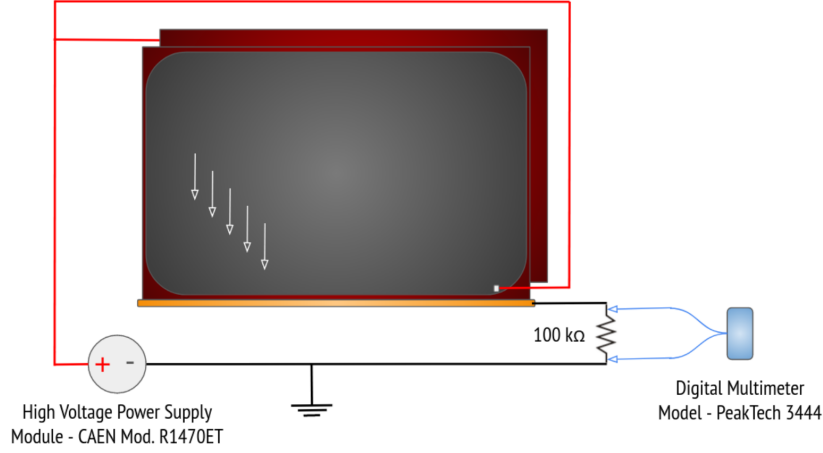
20

Figure 15: Diagram of the test stand used for leakage current measurement of a full-scale RPC gas volume.

to 4 kV, followed by 100 V increments up to the maximum operating voltage of 6.2 kV. Current measurements are performed through a 100 $k\Omega$ resistor connected between one of the HPL plates and ground, allowing accurate recording of the current flow. The applied high voltage V_{app} is corrected for local changes in environmental pressure P and temperature T at the production and certification facility by a high voltage correction factor to calculate the effective voltage V_{eff} using the equation:

$$V_{eff} = V_{app} \times \frac{P_0}{P} \times \frac{T}{T_0} \tag{4}$$

where $P_0 = 1010$ mbar and $T_0 = 293$ K are the reference temperature and pressure. The gap current is modeled as:

$$I_{gap} = \frac{V_{eff}}{R_{bulk}} + I_0 e^{\frac{V_{eff}}{V_0}} \tag{5}$$

where R_{bulk} represents the bulk ohmic resistance, I_0 is the mean primary charge produced per unit time, and V_0 depends on the gas mixture's effective Townsend coefficient. In the range of 0–3.5 kV, the current trend is predominantly ohmic, reflecting the bulk resistance. Above 4 kV, the current's exponential increase is driven by gas ionization effects. To meet quality standards, gas volumes are rejected if their leakage current exceeds 1 μA at 3.5 kV or if the exponential current exceeds 3 μA at 6.1 kV. This stringent
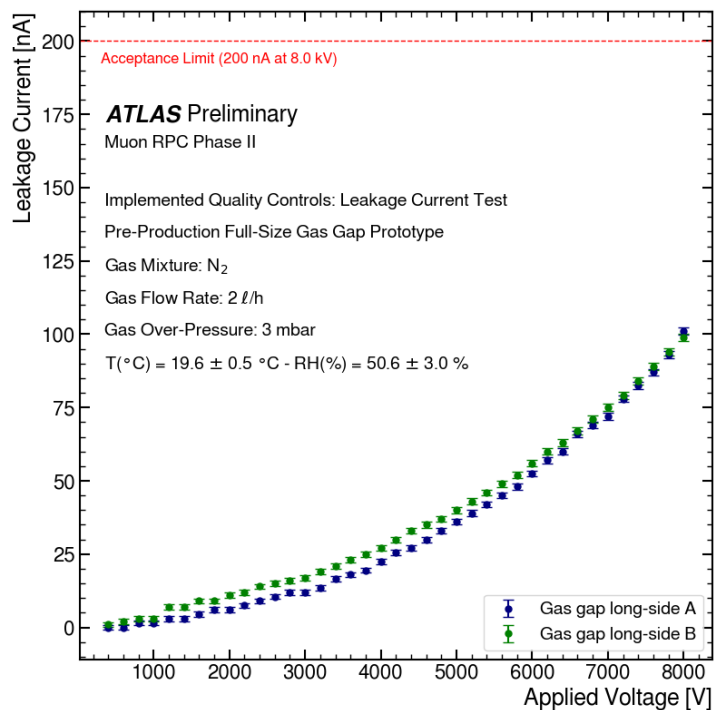
21

Figure 16: Leakage current test for a full-scale RPC gas volume.

criterion ensures that only volumes with minimal dark current and stable gas amplification advance to deployment. Representative results from the Volt-Amperometric characteristic test are presented in Figure 17.

5. RPC gas volume production facility at MPI

The production and certification facility for gas volumes has reached full operational status within the newly established clean room at the Max Planck Institute (MPI) building at the Garching Research Center. This state-of-the-art facility is designed to serve as a contingency site, ready to support or supplement production requirements should the primary German industrial facilities face any interruptions or increased demand. The MPI production center incorporates an advanced collaborative robotic system, enabling automation of critical steps in the gas volume assembly process. The robotic arm is equipped with integrated cameras, allowing real-time monitoring of the gluing phases directly at the application point. This video system de-
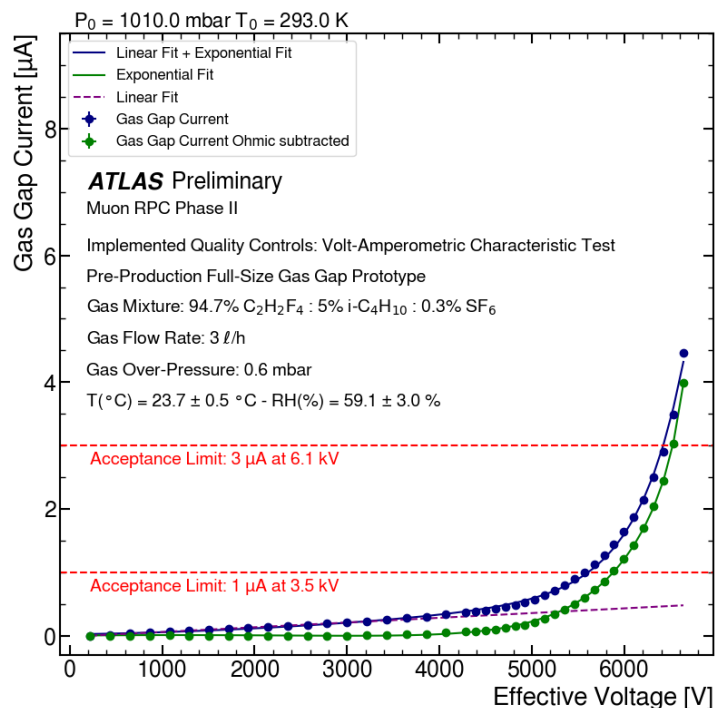
Figure 17: Volt-Amperometric characteristic test for a full-scale RPC gas volume.

tects any glue dispensing errors immediately, enabling prompt corrective actions to ensure high precision and reliability in assembly. Figures 18a and 18b show the freeze frames capturing the glue dispensing process during the assembly phase. The clean room provides a meticulously controlled environment, ensuring precise regulation of temperature and humidity - critical parameters for achieving high-quality gas volume bonding. Furthermore, this environment is indispensable for upholding the stringent standards of precision, cleanliness, and consistency required in gas volume assembly processes. Building on the expertise developed at MPI, industrial partners have been tasked with establishing an environment with controlled temperature and humidity to meet the stringent requirements of future series production of the gas volumes. Figure 18c shows a photograph taken inside the clean room at the Max Planck Institute during the assembly phase of a gas volume.

Figure 18: (a) and (b) Freeze frames capturing the glue dispensing onto the spacers (left) and along the side profiles (right) of the gas volume. (c) Assembly of a gas volume in the clean room at the Max Planck Institute. The controlled environment ensures precision and cleanliness in relevant production steps, critical to achieving high quality standards in gas volume construction.

6. Conclusion

The establishment of new industrial partnerships and production facilities for manufacturing Resistive Plate Chambers (RPCs) is a major step forward for the ATLAS Muon Spectrometer upgrade, preparing for the High-Luminosity LHC. By transferring advanced assembly techniques from research to industry and implementing scalable production processes, the team has shown that high-quality RPCs can be produced at an industrial scale.

Collaborations with German manufacturers PTS® and MIRION® and the Max Planck Institute ensured efficient production, while rigorous prototyping and certification confirmed the detectors meet high standards. These advancements represent a significant enhancement in RPC technology, benefiting current and future high-energy physics experiments.

References

[1] [ATLAS Collaboration], *Technical Design Report for the Phase-II Upgrade of the ATLAS Muon Spectrometer*, CERN-LHCC-2017-017.

[2] O. Kortner, H. Kroha, D. Soyk and T. Turković, *Optimization of the production procedures of thin-gap RPCs*, Nucl. Instrum. Meth. A **1053** (2023), 168273 doi:10.1016/j.nima.2023.168273.

[3] D. Pfeiffer *et al.*, *The radiation field in the Gamma Irradiation Facility GIF++ at CERN*, Nucl. Instrum. Meth. A **866** (2017), 91-103 doi:10.1016/j.nima.2017.05.045 [arXiv:1611.00299 [physics.ins-det]].

[4] T. Turkovic, *Production and Testing of Prototype Resistive Plate Chambers*, CERN-THESIS-2023-330.

[5] G. Aielli *et al.*, *Improving the RPC rate capability*, JINST **11** (2016) P07014 doi:10.1088/1748-0221/11/07/P07014 [arXiv:1606.03448 [physics.ins-det]].

[6] S. Park *et al.*, *Production of gas gaps for the Forward RPCs of the CMS experiment*, Nucl. Instrum. Meth. A **550** (2005), 551-558 doi:10.1016/j.nima.2005.05.052.